*Korean J. Chem. Eng.*, **16**(6), 823-828 (1999)

# Operation of Ceramic Candle Filter at High Temperature for PFBC Application

**Joo-Hong Choi†, Sang-Myung Keum and Jin-Do Chung***

Dept. of Chem. Eng. and RIIT, Gyeongsang National University, Chinju 660-701, Korea
*Dept. of Environ. Eng., Hoseo Univ., Asan 336-795, Korea
*(Received 6 May 1999 • accepted 6 September 1999)*

**Abstract**−In order to develop a reliable system of a ceramic filter for particulate collection at high temperatures like Pressurized Fluidized Bed Combustion (PFBC), an experimental study was carried out to observe the characteristics of the ceramic filter utilizing a simple block weigh-down. One block weigh-down fixes four commercial filter elements coincidentally by pressing down the individual venturi diffuser. Its operational performance was investigated in the temperature range of 600-800 °C in a bench scale unit using oil combustion gas into which fly ash was fed. The transient aspects of the temperature and pressure in the pulse cleaning system were also observed during the pulse cleaning.

Key words: Ceramic Filter, Particulate Collection, High Temperature, Transient Aspects

## INTRODUCTION

The ceramic candle filter is one of the most advanced technologies for the removal of particulates in PFBC and IGCC (Integrated Gasification Combined Cycle) [Lee et al., 1999] owing to its excellent removal efficiency and moderate operational cost. Unfortunately, the major problem in utilizing the ceramic filter is the uncertainty about the reliability of the system which has a high susceptibility for breakage of the filter element from several causes [Park et al., 1991]. Stresses caused by clamping, mechanical vibrations, and thermal cycle are the main sources which destroy both the filter element and the sealing materials. In order to reduce mechanical stress the filter element should be fixed tightly enough to overcome the cyclic forces developed during the filtration and the pulse cleaning. However, it is not easy to mount ceramic filter elements on the metallic tube sheet because they have different thermal expansibilities. In general, the tube sheet has an adequate hole in which the filter candle is mounted. The hole should have extra room to compensate for the expansion of metal parts at high temperatures. A ceramic gasket is placed between the metal and ceramic surface, which acts as a cushion and/or a sealing in this case. The compressible ceramic gasket may protect the candle element from damage enforced by uneven stresses due to the non-uniformities on the surface of the filter element [Mark and Stephen, 1995]. Extra force is needed to compress the gasket from the top of the filter element for sealing. Counter weight-down has been widely used with high temperature applications like PFBC [Grimethorpe PFBC Establishment, 1992]. Application of the spring is one of the methods to seal the leak parts while reducing the weight load from the weight-down itself. However, the metallic spring is susceptible to a reduction of its modulus at high temperature and under the corrosion gas. The utilization of the ceramic spiral spring was offered by the U.S. DOE [Ciliberti et al., 1988] in order to strengthen the spring. Another method involved welding the light hold-down disk on the tube sheet after specially setting up the filter element using a ceramic gasket [Ciliberti et al., 1988]. However, all of these methods are far from realization in the commercial unit yet. In this study, we applied mounting skill using a simple block weigh-down and investigated some operational characteristics. The block weigh-down is a steel plate which has holes to press down the diffuser. A block weight holds three or four filter elements and fixes the candle elements with its weight, which presses down the venturi diffuser. It provides stable pressure balances between filter elements and increases the reliability and durability of ceramic filters at high temperature owing to its simple features.

## EXPERIMENTAL

A schematic diagram of the experimental unit is shown in Fig. 1. The hot dusty gas stream was prepared with the oil burned-

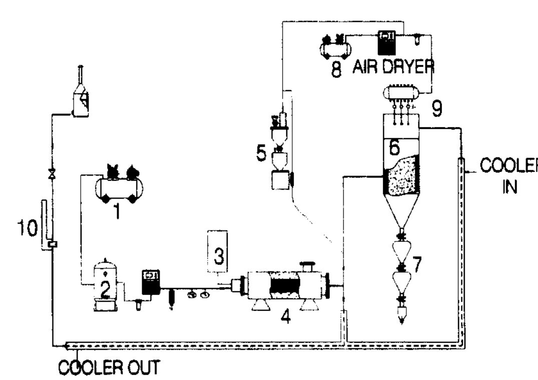


**Fig. 1. Schematic diagram of hot test unit for PFBC.**

| | |
|---|---|
| 1. Air compressor | 6. Filter unit |
| 2. Reservoir tank | 7. Dust hopper |
| 3. Oil tank | 8. Pulse air compressor |
| 4. Oil burner | 9. Pulse gas tank |
| 5. Dust feeder system | 10. Orifice |

†To whom correspondence should be addressed.
E-mail: jhchoi@nongae.gsnu.ac.kr

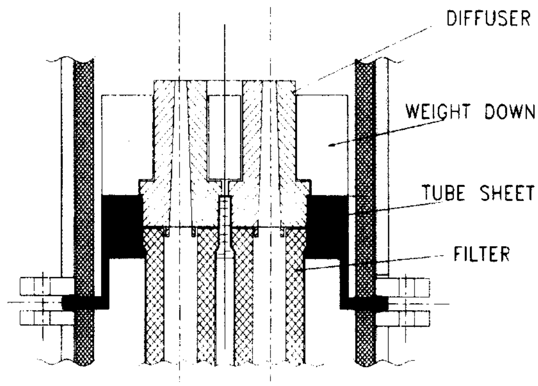


**Fig. 2. The schematic diagram of the filter candle assembled.**

exhaust gas in which the fly ash from a conventional coal power plant was fed with a screw feeder. The inlet gas enters the filter chamber from the bottom position. The temperature in the filter unit was controlled with the change of the oil feeding rate. The range of operating temperature was between 600 and 800 °C. Total filtration area is 1.04 $m^2$ using four candle elements of 1.5 m length. The inner diameter and height of filter chamber are 280 and 2,800 mm, respectively. Fig. 2 shows the assembled figure of filter candles on the tube sheet. The tube sheet has four holes which allow the insertion of filter elements. Four filter elements were fixed by the weight of one block weight-down. Each filter element was cleaned by each nozzle. The size of the cylindrical pulse air tank of inner diameter and length is 223 and 550 mm, respectively. A half-inch solenoid valve (direct lift diaphragm) was used as the pulse valve, of which the coefficient was 4.5 *l*/bar · sec.

The total pressure drop between the tube sheet was measured with a differential pressure transmitter. Temperatures and pressures were measured at several points in order to investigate the transient phenomena. The dust concentration was measured with a gasket impactor or an aerodynamic particle size analyzer. The commercial filter candle based on ceramically bonded silicon carbide was supplied by Schumacher Co. and has a dimension of 1.5 m length and 6 cm outer diameter. Its physical properties were reported well in another paper [Durst et al., 1996].

**Table 1. Operation conditions and performance of a hot bench ceramic filter unit**

| Operating conditions | | Performances | |
|---|---|---|---|
| Operating temperature | 600-800 °C | Face velocity | 1-5 cm/sec |
| Nozzle tube | 1/2 inch | Slip particle size (max.) | less than 5 μm |
| Particulate loading | 20-40 g/$m^3$ | Total filtration efficiency | more than 99.9% |
| Pulse pressure | 5-9 bar | Duration (continuous) | 60 hr |
| Pulse duration | 0.1-0.6 sec | Duration (accumulated) | 1,500 hr |

## RESULTS AND DISCUSSIONS

### 1. Performance

The operating conditions and the performance of the filter system are summarized in Table 1. The typical filtration efficiency of the test unit was more than 99.9% during the continuous duration of 60 hours at 750 °C. Most of larger particles over 3 μm were removed. And the maximum particle size leaked through the filter was less than 5 μm. This result shows that the ceramic filter system designed using the block weigh-down meets the requirements of the specifications for PFBC. The largest slip size of particle and the total concentration of particles in the effluent gas stream should be less than 5 μm and 10 ppm, respectively, for advanced power systems [Choi et al., 1995]. Pressure drop through the hollow cylinder is well expressed by Darcy's law like Eq. (1), where $\eta$ is dynamic viscosity and V is face velocity.

$$\Delta P = \frac{\eta V}{k} \tag{1}$$

Permeability k indicates the capacity of the gas treatment per unit pressure drop. It decreases as the dust cake gets thicker with the operation time. Thus, the relative permeability K, which indicates the relative value from that of the initial time (denoted by subscript zero in the equation) like Eq. (2), is very convenient for predicting the permeability change [Durst et al., 1996].

$$K = \frac{k}{k_0} = \frac{V \cdot \eta / \Delta P}{V_0 \cdot \eta_0 / \Delta P_0} \tag{2}$$

Fig. 3 shows a typical pattern of the variation of the relative permeability during the very short duration as a function of cycle duration. K decreases rapidly during the initial time and reaches a stable point ultimately in the suitable operation conditions.

The trend of the baseline pressure drop ($\Delta P_B$) is one of the factors which represent the performance of the filtration. In general, the design value of the tolerance limit of $\Delta P_B$, depending on the system and operating conditions, is about 2,000 $mmH_2O$ [Grimethorpe PFBC Establishment, 1992]. Fig. 4 shows the trend of the increase of the base line pressure drop accord-

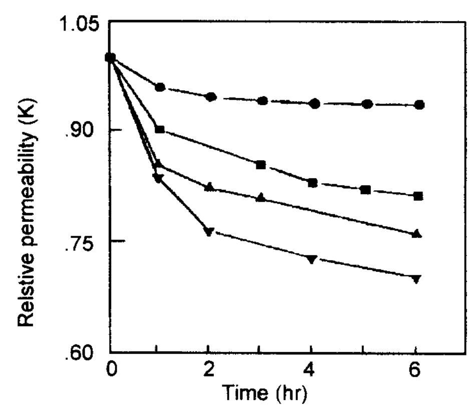


**Fig. 3. The decrease of relative permeability with the pulse cycle duration; ●(5), ■(10), ▲(15) and ▼(20 min).**

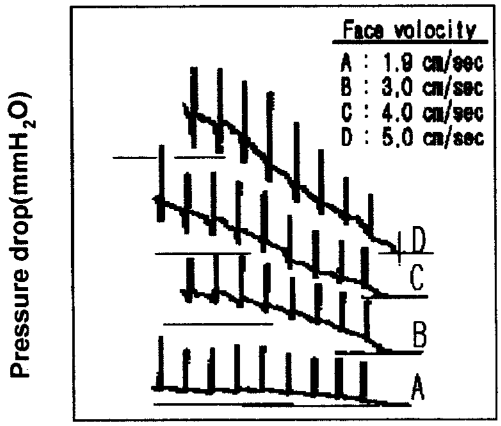


**Fig. 4. The trend of pressure drop depending on the face velocity (One pulse cycle is it minutes).**

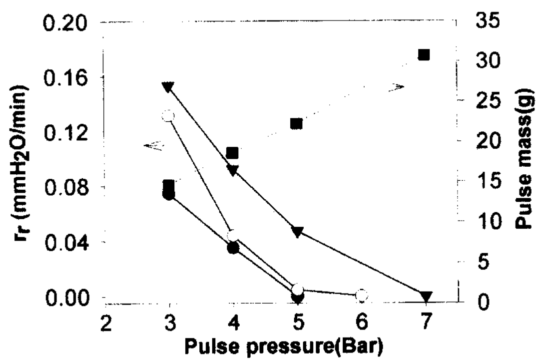


**Fig. 5. The effect of face velocity on the residual pressure drop rate [Face velocity: 1.5 (●), 2.7 (○) and 4.0 cm/sec (▼) and pulse mass (■)].**

ing to the face velocity. And its operations are summarized in Table 2. $\Delta P_F$ in the table represents the pressure drop through the clean filter element. The baseline pressure drop increased steeply when the face velocity was higher than 4 cm/sec and was not recovered with the pulse cleaning at a pulse pressure of 4 bar. It is evident that the pressure drop increases as both the face velocity and the temperature increase according to Darcy's law because the gas viscosity increases with the temperature. However, a face velocity of 4 cm/sec is not so high in the general operation condition for PFBC. The reason why the operation showed a malfunction in this test is due to the inlet position which lies at the bottom of the filter unit. It seems that most of the particulate falling down during the pulse cleaning is entrained by the force of the entering gas, of which the flow direction is from bottom to top. So the filter system having the

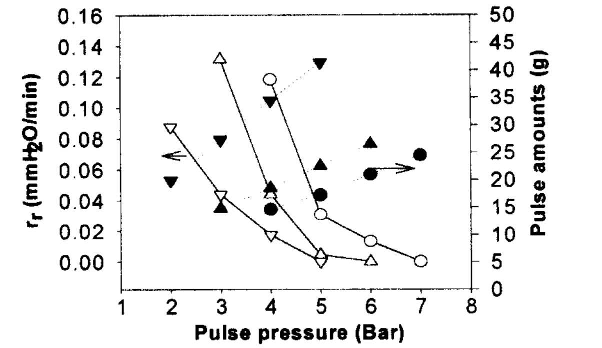


**Fig. 6. The dependence of pressure drop rate on the pulse condition when face velocity is 2.71 cm/sec [Pulse duration (mass & $r_r$): 0.1 (● & ○), 0.2 (▲ & △) and 0.6 (▼ & ▽)].**

inlet position at the bottom was not desirable for operation at high face velocity. Fig. 5 shows the effect of the face velocity on the residual pressure drop rate which is defined by Eq. (3).

$$r_r = \frac{d\Delta P_R}{dt} \quad (3)$$

Where $\Delta P_R$ is the residual pressure drop and t is time. The pulse mass, calculated from the pressure difference of the pulse tank during the pulse cleaning, increased linearly with that of the pulse pressure. The value of $r_r$ reached zero when a high value of pulse pressure was applied even in the case of face velocity of 4 cm/sec. However, applying the strong pulse gas should cause a mechanical stress and need the unnecessary pulse energy.

Among the several operation variables, pulse pressure and pulse duration are the main factors. Fig. 6 shows the effect of pulse pressure and pulse duration on the residual pressure drop rate. It shows the value of $r_r$ reaches zero at the higher value of pulse pressure depending on the pulse duration. The higher the pulse pressure and the lower the pulse duration, the less the pulse mass is consumed in order to achieve the zero value of $r_r$. This result suggests that it is profitable to apply as high a pressure of the pulse gas as possible. However, the high value of the pulse gas may be one of the reasons for the mechanical stress in the filter mounting system and a non-equilibrium pressure drop in the filter cavity during the pulse cleaning.

**2. Temperature Distribution**

In order to observe the temperature distribution during the pulse cleaning, we measured the transient temperatures in the pulse cleaning system and the filter cavity. A bared-thermocouple of type K (CA) was used. Their dimension and the loca-

**Table 2. The operation conditions and the effect of face velocity on the pressure drop through the filter element**

| Mark | Operation temp. (°C) | Face velocity (cm/sec) | Pulse P (Bar) | Pulse duration (Sec) | Pulse cycle (min) | $\Delta P_F$ ($mmH_2O$) |
|---|---|---|---|---|---|---|
| A | 250 | 1.9 | 4 | 0.4 | 5 | 115 |
| B | 435 | 3.0 | 4 | 0.4 | 5 | 160 |
| C | 545 | 4.0 | 4 | 0.4 | 5 | 240 |
| D | 640 | 5.0 | 5 | 0.4 | 5 | 260 |

**Table 3. The description of temperature measurement**

| Notation | Location | Measuring range (°C) | Thermocouple fitting, Length | Response time (ms) |
|---|---|---|---|---|
| TNZ | Nozzle tip | 200-900 | 1/16 inch, 700 mm | 20 |
| TCT | Cavity top | 200-900 | 1/16 inch, 1,500 mm | 20 |
| TCM | Cavity middle | 200-900 | 1/16 inch, 2,000 mm | 20 |
| TCB | Cavity bottom | 200-900 | 1/16 inch, 2,500 mm | 20 |

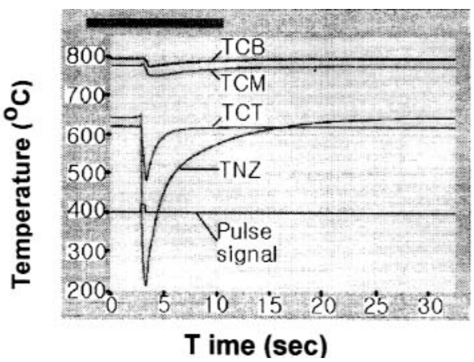


**Fig. 7. The temperature traces during the pulse cleaning.**

tions of measuring points are shown in Table 3. Steady state temperatures at the cavity middle (TCM), cavity top (TCT), clean chamber (TTC), and tube sheet surface (TTS) were 775, 640, 570 and 510, respectively, when the temperature in the filter chamber (TFM) was 800 °C. The enormous temperature drop of about 230 °C between the filter chamber and the clean chamber comes from the heat loss through the wall of the clean chamber where the thermal insulation is insufficient.

Fig. 7 shows the typical temperature traces at the positions along the filter cavity and in the nozzle tip when TFM is 800 °C. The face velocity, the pulse pressure and the pulse duration were 5.2 cm/sec, 5 bar, and 0.4 sec, respectively. The highest temperature drop was developed in the cavity top and was about 200 °C depending on the pulse pressure shown at Fig. 8.

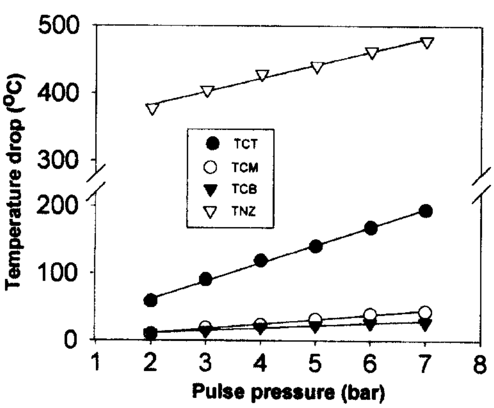


**Fig. 8. The temperature drop during the pulse cleaning (Face velocity: 5.2 cm/sec, Pulse duration: 0.4 sec).**

**Table 4. The description of pressure measurement**

| Notation | Location | P range | Signal output | Response time (ms) |
|---|---|---|---|---|
| PPT | Pulse tank | 0-10 bar | 4-20 mA | 10 |
| PNZ | Nozzle tip | 0-10 bar | 4-20 mA | 10 |
| PCM | Cavity middle | 0-30 psig | 4-20 mA | 10 |
| PFM | Filter chamber | 0-30 psig | 4-20 mA | 10 |

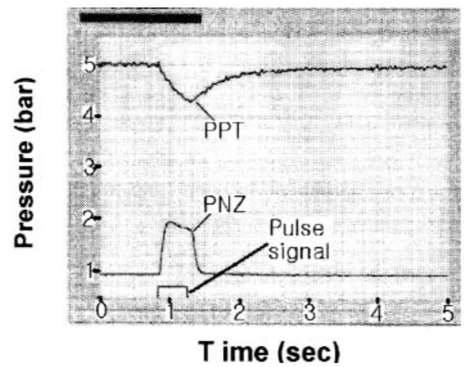


**Fig. 9. The pressure traces in the pulse system during the pulse cleaning.**

Even though the temperature drop in the filter cavity does not represent directly the just temperature drop in the filter element, it is a fact that the periodical thermal cycle will be one of the serious reasons for the thermal stress on the filter element. Temperature drop in the bottom and middle positions of the filter cavity was relatively ignored. This result predicts that most of the cold pulse gas is expanded and heated in the top area of the filter cavity; and this area is just the site that is very susceptible to thermal cracking. Temperature drop in the nozzle was more than 400 °C, as shown at Fig. 7. So it is predicted that there will be high thermal fatigue in the pulse nozzle.

**3. Pressure Distribution**

The transient pressure change during the pulse cleaning in the pulse system and the filter cavity was measured at the positions shown in Table 4.

Fig. 9 shows the typical patterns of pressure traces in the pulse tank and the pulse nozzle during the pulse cleaning when the pulse pressure and the pulse duration are 5 bar and 0.4 sec, respectively. The pressure in the pulse tank was recovered within one second. Pressure dropped from 5 bar to 4.3 bar, which showed about 10% reduction of pressure in the pulse gas tank. About 1.0 bar of the overpressure was developed in the pulse nozzle. However, the intensity of the overpressure is fully dependent on the size of the pulse system and the operation conditions.

Fig. 10 shows the typical pressure traces at both the filter cavity and the filter chamber during the pulse cleaning. The positive differential pressure, overpressure, denotes the effectiveness of the pulse cleaning which supplies the main momentum for the dust removal from the filter surface. The plateau denoting the overpressure in the filter cavity increased slightly at the end of the pulse duration. This is because the post cleaned-gas

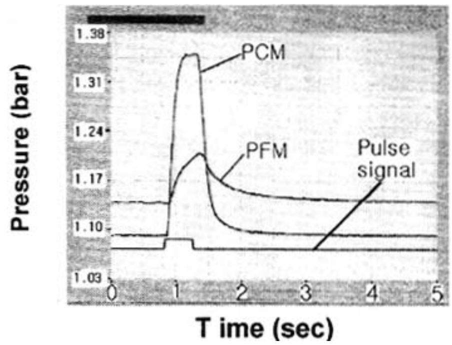


**Fig. 10. The pressure traces in the filter cavity during the pulse cleaning.**

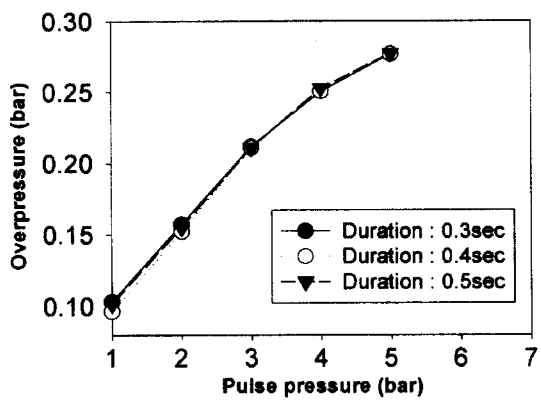


**Fig. 11. The dependence of the pulse pressure on the overpressure in the filter cavity during the pulse cleaning.**

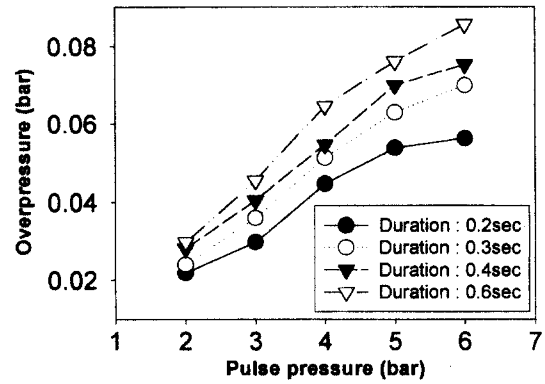


**Fig. 12. The effect of the pulse pressure on the overpressure in the filter chamber.**

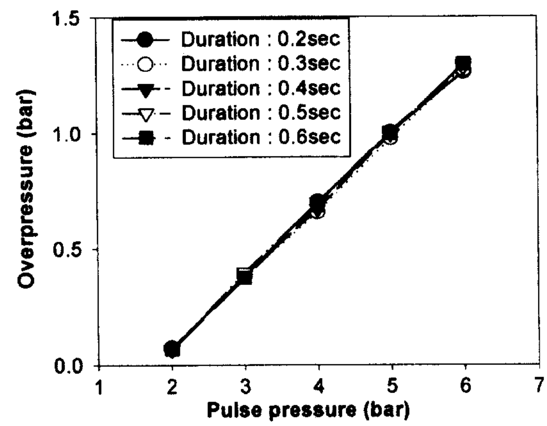


**Fig. 13. The effect of the pulse pressure on the overpressure in the pulse nozzle.**

entering after the pulse cleaning stimulates the formation of the positive pressure effect. The overpressure developed in the filter cavity was about 0.248 bar when the pulse pressure was 5 bar. This effect of pressure is sufficient for removing the dust cake in normal operation conditions as shown at Fig. 5 and Fig. 6. The background pressure in the filter chamber was apparently increased from the expansion of the pulse gas, which means the space of the filter chamber is relatively small with respect to the pulse gas. In this experimental system, 25% of filter element was cleaned by every pulse cleaning. The effect of the pulse gas will be ignored in a commercial plant where about 5% of filter elements are cleaned per pulse cleaning.

Fig. 11 shows the maximum overpressure in the candle cavity increases linearly with the pulse pressure at low pressures below about 4.5 bar. But its increasing rate decreases slightly at high pressure. The increasing tendency of the overpressure in the filter chamber shows a similar pattern with this as shown in Fig. 12. So the slight decrease of the overpressure at high pressure comes from the reduction of pulse gas entering the filter cavity even though the overpressure in the pulse nozzle increases linearly with the pulse pressure as shown in Fig. 13. The reason is that the velocity through the pulse nozzle does not increase after it reaches the super sonic velocity. However, the slight increase comes from the increase of the gas density at slightly high pressure at high pulse pressure. The experimental result supporting this discussion was shown in another paper [Choi et al., 1998]. The effect of the pulse duration on the maximum overpressure both in the filter cavity and in the pulse nozzle was ignored as shown in Fig. 11 and Fig. 13, respectively.

## CONCLUSIONS

The performance of the ceramic filter unit utilizing a block weigh-down was investigated in the range of 600-800 °C using oil burned-exhaust gas. The normal filtration efficiency was more than 99.9%. The largest particle size which slipped from the filter was less than 5 µm. The pressure drop showed a normal trend of a general ceramic filter during continuous operation of 60 hours. These results show that the mounting skill of the filter element using a block weigh-down meets well with the specifications for PFBC.

The development of overpressure in the filter cavity was less than 0.21 bar at the normal operation conditions. The highest temperature drop developed in the top cavity of the filter element. Temperature drop in the pulse nozzle was more than 400 °C at normal operation conditions. So it was predicted that the high thermal stresses were concentrated both in the pulse nozzle and in the top area of the filter cavity.

## ACKNOWLEDGEMENT

This paper was supported by R&D Management Center for Energy and Resources. Authors appreciate its financial support.

## REFERENCES

Clift, R., Seville, J. P. K. and Kuile, J. W. W., "Rigid Ceramic Media for Filtering Hot Gases," Filtration & Separation, July/August, 265 (1989).

Ciliberti, D. F., Boro, M. and Lippert, T. E., "Filter Unit for Use at High Temperatures," U S Patent 4,735,638, April 5 (1988).

Choi, J. H., Ji, P. S. and Chung, J. D., "Technical Evaluation of Current HTHP Gas Particulate Collectors for IGCC," Proceedings of The 3rd International Symposium on COAL COMBUSTION- Science and Technology, September 8-21, Beijing, China, 514 (1995).

Choi, J. H., Park, K. W., Keum, S. M. and Chung, J. H., "Measurement of Transient Phenomena During the Pulse Cleaning of the Ceramic Filter Unit," Proceedings on Second Korea-China Joint Workshop on Coal & Clean Energy Utilization Technology, Taejon, Koera, November 2-6, 167 (1998).

Durst, M., Freude, E., Schulz, K. and Walch, A., "Schumacher's Hot Gas Filter Technology," Private report, March (1996).

Grimethorpe PFBC Establishment, "Grimethorpe High Temperature High Pressure Gas Filter Experiment Program," EPRI TR-100499, **2**, 3 (1992).

Lee, S. J., Lee, J. W., Kim, Y. C. and Yun, Y., "Performance Evaluation of the IGCC Process Development Unit System," *HWAHAK KONGHAK*, **37**, 47 (1999).

Mark, W. J. and Stephon, A. G., "Filter Assembly Having a Filter Element and a Sealing Device," U S Patent 5,401,406, Mar. 28 (1995).

Park, Y. O., Ghim, Y. S., Son, J. E. and Chung, T. S., "Coal Fly Ash Collection by Glass Fabrics-I. Growth of Dust Deposition and Pressure Drop Characteristics," *HWAHAK KONGHAK*, **29**, 463 (1991).